Theoretical study of the filling fraction limits for impurities in $CoSb_3$

X. Shi,[1,2] W. Zhang,[1] L. D. Chen,[1] J. Yang,[3] and C. Uher[2]
[1]*State Key Laboratory of High Performance Ceramics and Superfine Microstructure, Shanghai Institute of Ceramics, Chinese Academy of Sciences, Shanghai 200050, China*
[2]*Department of Physics, University of Michigan, Ann Arbor, Michigan 48109, USA*
[3]*Materials and Processes Laboratory, General Motors R&D Center, Warren, Michigan 48088, USA*
(Received 17 November 2006; revised manuscript received 17 March 2007; published 29 June 2007)

The filling fraction limits (FFLs) of various impurities for the intrinsic voids in the lattice of $CoSb_3$ are studied by combining the density functional method and thermodynamic analysis. The FFL for the voids is shown to be determined by both the interaction between the impurity and the host atoms and the secondary phase formation ability of the impurity atoms with one of the host atoms. The FFLs predicted for impurities Ca, Sr, Ba, La, Ce, and Yb in skutterudite $CoSb_3$ agree very well with the experimental values. Several models are proposed to explain the various formation energies quantitatively, which unveil the physics behind the FFLs. The correlation between various energies and chemical bonding, lattice strain, and the effective charge state of impurities is investigated systematically. A simple selection rule for forming stable filled skutterudites is discovered, and it agrees with the experimental observations.

DOI: 10.1103/PhysRevB.75.235208 PACS number(s): 61.72.Bb, 72.15.Jf

I. INTRODUCTION

$CoSb_3$-based skutterudites are among the most important thermoelectric materials that have been studied extensively in recent years.[1] The chemical formula of a binary skutterudite is MX_3, where the metal atom M can be Co, Rh, or Ir, and the pnicogen atom X can be P, As, or Sb. Binary skutterudite compounds crystallize in a body-centered-cubic structure with space group $Im3$ and have interstitial voids at the $2a$ positions (12-coordinated) in the lattice. Each M atom is octahedrally surrounded by X atoms forming a MX_6 octahedron. Binary $CoSb_3$ is a semiconductor with small band gap ($\sim$0.5 eV), high carrier mobility, and modest thermopower. However, it also possesses high thermal conductivity values ($\sim$10 W/m K at room temperature) that limit its thermoelectric performance.

It has been proven to be an effective way of reducing the lattice thermal conductivity of $CoSb_3$-based skutterudites to fill the lattice voids with impurity atoms to form partially filled skutterudites $I_yCo_4Sb_{12}$, where I represents an impurity atom and y is its filling fraction.[1] The filler atoms show large atomic displacement parameters, rattle inside the 12-coordinated sites surrounded by Sb atoms, interact with low-frequency lattice phonons, and significantly reduce the lattice thermal conductivity of filled skutterudites. The reduced thermal conductivity results in a substantial improvement of thermoelectric performance at elevated temperatures. The demonstration of thermal conductivity reduction over a wide temperature range due to the presence of fillers was first reported in Ce-filled skutterudites.[2] Subsequently, similar effects were observed in skutterudites filled with various other filler atoms.[1] $CoSb_3$-based filled skutterudites with various filler atoms (Ce, La, Nd, Eu, Yb, Tl, Sn, Ge, Ca, and Ba) without charge compensation have been intensively studied in an effort to search for better n-type thermoelectric materials. Currently, the best experimental values of the thermoelectric figure of merit ZT are in the range of 1–1.3 at elevated temperatures.[3–12]

The filling fraction of filler atoms in skutterudites greatly influences both the electrical and thermal transport.[1–12] Experimentally it was found that there exists a maximum filling fraction for each impurity in the host skutterudite structure.[3–12] It is, however, not clear whether the maximum filling fraction is really a filling fraction limit (FFL) intrinsic to the impurity or a value determined inadvertently by extrinsic factors. It is believed that the FFL is controlled simultaneously by several factors such as the valence state, the electronegativity, and the atomic radius of the filler. It is evident that filling the crystal structure voids results in a drastic reduction of the lattice thermal conductivity, and that the concomitant effect of doping is very beneficial to thermoelectric properties. The existence of the FFL in the host skutterudite structure, however, limits further reduction of the lattice thermal conductivity.

Theoretical aspects of skutterudites have been studied in numerous previous works. For example, CoP_3 and NiP_3 have been studied by using the linear muffin-tin orbital method in the atomic sphere approximation.[13] Singh and co-workers have used the linearized-augmented-plane-wave method within the local-density approximation to calculate various properties of $IrSb_3$, $CoSb_3$, $CoAs_3$, CoP_3, $LaFe_4P_{12}$, and $(La,Ce)Fe_4Sb_{12}$.[14–16] Løvvik *et al.* and Bertin *et al.* have investigated the thermodynamic stabilities and some electronic properties of CoP_3- and $CoSb_3$-based filled skutterudites, respectively.[17,18]

In our previous work, the FFLs for Ca, Sr, Ba, La, Ce, and Yb filled skutterudites have been studied by density functional theory, and the most important results have already been reported.[19] This paper represents an extension of the work on the FFL problem. After a brief overview of computational details and summary of the method that leads to FFL, we mainly focus on the physical understanding of the FFL problem in detail.

II. COMPUTATIONAL DETAILS

The projector-augmented-wave (PAW) method,[20] as implemented in the Vienna *ab initio* simulation package (VASP),[21] is utilized for this study, which uses a plane-wave

basis set for the expansion of the single-particle Kohn-Sham wave functions. The Perdew-Burke-Ernzerhof generalized gradient approximation (GGA)[22] for the exchange-correlation potential is used for all the calculations. Extensive tests by us and others have shown the effectiveness of the VASP package,[19,23,24] a popular plane-wave electronic structure calculation program. The criterion used for self-consistency in the electronic structure calculations was that two consecutive total energies differed by less than 0.0001 eV. All calculations are performed using the cutoff energy as high as 350 eV for the plane-wave basis set, $1\times1\times1$ Monkhorst-Pack uniform k-point sampling for integrals over the Brillouin zone of filled $CoSb_3$ to save computational time, and $4\times4\times4$ Monkhorst-Pack uniform k-point sampling for other compounds. Smearing factor of 0.1 eV is used for the Fermi integral. Switching the smearing factor from 0.1 eV to 0.05 eV and then to 0.02 eV at $1\times1\times1$ k points and the 132-atom supercell approach for $Ba_{0.5}Co_4Sb_{12}$ (50% filling) system affect slightly the total energies of the filled system and related phases. In addition, those only change the defect formation energies ΔH_1 (see Sec. III) by about 0.01 eV. Switching the k points from $1\times1\times1$ to $2\times2\times2$ and then to $4\times4\times4$ for the filled supercell with smearing factor of 0.1 eV only leads to the change of ΔH_1 by about 0.02 eV. So, it is reasonable to assume that the numerical error in our calculations is very small. The ionic coordinates and the unit cell size were optimized simultaneously to eliminate structures with internal stress. A structure was considered relaxed when all the forces exerted on atoms were less than 0.01 eV/Å. A single calculation using high accuracy was performed after the completion of the structure relaxation to obtain the total free energy.

The skutterudite structure contains two large intrinsic voids in the conventional unit cell (Fig. 1). Within one unit cell, there are three different ways for impurities to fill the voids, and the corresponding filling fractions are 0, 0.5, and 1. These do not match well the experimental FFL values between 0 and 0.44. To ensure a direct comparison with the experimental results, all calculations were carried out in a supercell ($2\times2\times2$ primitive cell) with a total of 128 atoms and eight voids of pure $CoSb_3$ (see Fig. 1). There are altogether nine different filling fractions as listed in Table I, and more than one possible filling configuration for each filling fraction. For each possible filling configuration, the corresponding number of different total energies due to various filler distributions in the voids of the host skutterudite structure is also listed in Table I. Electronic structures for all these configurations are calculated and the ones with the lowest total energy are employed for further analysis.

III. RESULTS AND DISCUSSION

The method for determining the FFL in filled skutterudites has been given in Ref. 19. Briefly, we demonstrated that the FFL is determined by the competition between the formation of a filled skutterudite and that of secondary phases, i.e.,

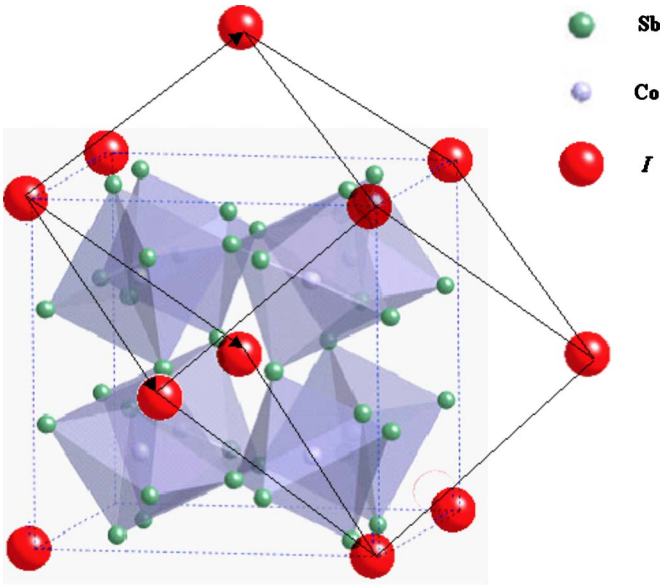

FIG. 1. (Color online) The conventional unit cell (dotted line) and the primitive cell (solid line) of the skutterudite structure. All calculations for filled $CoSb_3$ were done with a $2\times2\times2$ supercell of the primitive cell.

$$nI + 4CoSb_3 \rightarrow \frac{(2-n)}{(2-y)}I_yCo_4Sb_{12} + \frac{2(n-y)}{(2-y)}ISb_2 + 4\frac{n-y}{(2-y)}CoSb_2. \quad (1)$$

The Gibbs energy of reaction (ΔG_3) for the above equation can be expressed as a combination of that for forming filled skutterudites (ΔH_1) and that for forming secondary phases (ΔH_2). The FFL of an impurity corresponds to the filling fraction y that gives rise to the minimum of ΔG_3. It was shown that the calculated FFLs are in good agreement with the experimentally measured ones for Ca,[9] Sr,[25] Ba,[10] La,[4] Ce,[3] and Yb[7] in $CoSb_3$. Readers who are interested in this problem may go to Ref. 19 for details.

A. Interaction between filler atoms and crystal environment in $CoSb_3$

Details on the definitions and analysis of the impurity formation enthalpy (ΔH_1), the formation energy of an isolated impurity (ΔE_1), the interaction energy between impurity atoms (ΔE_2), and the formation energy of the secondary phases were given in Ref. 19. By expressing $\Delta H_1 = \Delta E_1 + y\Delta E_2$, the FFL of an impurity in $CoSb_3$ can be given analytically at 0 K as[19]

$$y_{max} = 2\left(1 - \sqrt{1 + \frac{\Delta E_1 - \Delta H_2}{2\Delta E_2}}\right), \quad (2)$$

or

$$y_{max} - \frac{y_{max}^2}{4} = \frac{\Delta H_2 - \Delta E_1}{2\Delta E_2}. \quad (3)$$

TABLE I. Possible configurations for impurities occupying the eight voids in a $2\times2\times2$ $CoSb_3$ supercell and the corresponding number of different total energies.

Filling fraction	0	12.5%	25.0%	37.5%	50.0%	62.5%	75.0%	87.5%	100.0%
Possible configurations	1	1	3	3	5	3	3	1	1
Number of different energies	1	1	2	2	2	2	2	1	1

According to Eq. (2), the FFL is determined by three parameters: ΔE_1, ΔE_2, and ΔH_2. The impurity atom can fill the voids in $CoSb_3$ only when $\Delta E_1 < \Delta H_2$. A high FFL requires a low formation energy of an isolated impurity in $CoSb_3$, high formation energies of secondary phases, and a small interaction between impurity atoms. The interplay amongst these various energies determines y_{max}.

1. What determines ΔE_2?

Physical analysis leads us to express ΔE_2 as a screened Coulombic interaction [Eq. (5) in Ref. 19] between impurities with an effective charge state q_I, the number of lost electrons when filling into the voids in $CoSb_3$. The estimated effective charges are listed under q_I in Table II. The charge states of all impurities in $CoSb_3$ can also be estimated by integrating the density of states (DOS) of the filled $CoSb_3$ system up to the Fermi level. The DOS is readily obtainable from electronic structure calculations, and the effective charges from the DOS integrals are also listed in Table II. The effective charge states calculated by these two methods show good agreement. More importantly, a perfect linear dependence of ΔE_2 on the q_I^2 is also obtained. Therefore, it is reasonable to conclude that q_I can be taken as the real valence charge of the impurity in $CoSb_3$. In fact, our calculated q_I values do agree reasonably well with the experimental ones estimated based on carrier concentration measurements,[3–10,26] which are also listed in Table II.

Equations (2) and (3) show that a lower ΔE_2 corresponds to a higher FFL. Therefore, a lower valence charge state of an impurity is likely associated with a higher FFL. Both the measured and the calculated data show that Ba and Sr have effective valences of +2, lowest among all the impurities studied in this paper, in agreement with their high FFL values ~40%. In fact, Ba has the highest FFL amongst all impurities that have been studied so far. Ce has a relatively higher valence charge state between +2.5 and +3, which is also consistent with its relatively low FFL ~10%.[3]

TABLE II. Effective charges for various impurities in $CoSb_3$ determined by Eq. (10), electronic density of state (DOS), x-ray absorption near edge spectroscopy (XANES), and experimental carrier concentration (n).

q_1	Ca	Sr	Ba	La	Ce	Yb
Eq. (10)	1.86	1.94	2	2.82	2.51	1.73
DOS	1.9	2	2	2.75	2.49	1.76
XANES						2.45[a]
n	1.87[b]		2[c]	2.91[d]	2.4–2.9[e]	

[a]Reference 26.
[b]Reference 9.
[c]Reference 10.
[d]Reference 4.
[e]Reference 3.

2. Effective charge states of impurities in $CoSb_3$

Because impurities in this study are metals, they have the tendency to lose their valence electrons after being inserted into the voids of the lattice. The valence electrons of the filler atom, however, are not completely transferred to the neighboring Sb atoms, because the chemical bonds between impurity and Sb atoms are not purely ionic. Hall measurements on some filled skutterudites also indicate that valence electrons of the filler atom are not completely lost. For example, the estimated charge state deduced from the measured carrier concentration is between +2.4 and +2.9 for Ce,[3] +2.91 for La,[5] +1.87 for Ca,[9] and +2 for Ba.[10]

The valence charge state +2 of Ba is chosen, in this study, as a reference due to its well-defined ionized state for nearly all Ba-containing compounds.[27] XPS measurements for $Ba_yCo_4Sb_{12}$ compounds[28] and related systems[17] also show that the valence state for Ba in $CoSb_3$ is +2. Thus the effective charges of other impurities in $CoSb_3$ can be obtained using Eq. (5) in Ref. 19, with the value of ΔE_2 obtained from fits to Eq. (7). The calculated effective charges are listed in Table II.

The charge states of the impurities are also estimated by integrating the calculated electronic density of states (DOS) to the Fermi level. Figure 2 shows the projected density of states for the impurities in filled $CoSb_3$. The states of 4s electrons for Ca, 5s electrons for Sr, and 6s electrons for Ba are all above the Fermi level, indicating that all the outer s electrons are stripped off. It is, therefore, obvious that the effective charge states for Ca, Sr, and Ba in filled $CoSb_3$ should be close to +2. The electronegativity value of Ca is larger than those of Sr and Ba, and thus, the covalent portion of the Ca-Sb chemical bonds should also be the highest amongst the three alkaline earths. The effective charge for Ca is, as expected, slightly smaller than those of Sr and Ba (Table II). According to Fig. 2, all 6s electrons for La in $CoSb_3$ are stripped off and one 5d electron is almost lost with some 5d orbitals below the Fermi level, indicating that the effective charge of La is smaller than, but close to +3. The density of states for Ce in $CoSb_3$ is similar to that for La. The electronegativity value of Yb is close to those of La and Ce; all 4f energy levels and a few 6s energy levels of Yb are below the Fermi level as shown in Fig. 2. Based on our calculations using the projected DOS, the effective charge of Yb in $CoSb_3$ is less than +2, consistent with the previous estimates using ΔE_2. It, however, does not agree with the

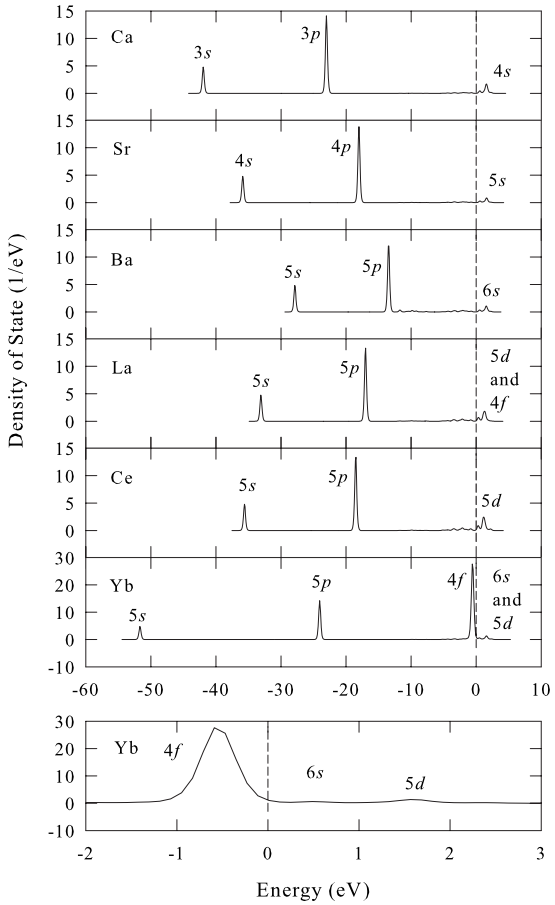

FIG. 2. Projected density of states (DOS) of the filler atoms in filled $CoSb_3$. Dashed lines represent the Fermi level.

value obtained by XANES measurement.[26] We do not know the exact cause of this discrepancy, but plan to investigate it in the future.

Effective charges of impurities in $CoSb_3$ estimated by various methods, listed in Table II, are generally in good agreement. Therefore, it is reasonable to conclude that the effective charges can be taken as the real valence charges of impurities in filled $CoSb_3$. These values are also consistent with the picture that the interaction between an impurity and host $CoSb_3$ material is predominantly ionic in nature.

3. What determines ΔE_1?

When impurity atoms are inserted into the voids of $CoSb_3$ to form a filled skutterudite, the crystal lattice is expanded. At the same time, these impurity atoms lose their valence electrons and form bonds (interact) with the surrounding host atoms. In addition, the interaction may change the original positions of the host atoms. ΔE_1 is defined as the formation energy of an isolated impurity defect.[19] There are two parts that contribute to ΔE_1. One is from the strain effect, i.e., the lattice expansion and structure deformation due to the insertion of an impurity into the lattice void of $CoSb_3$. Another arises because of the extra chemical bonding formed between the filler atom and the surrounding $CoSb_3$ lattice environment. We can write ΔE_1 as

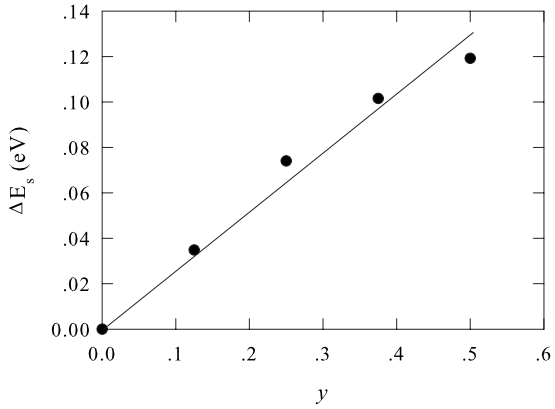

FIG. 3. Strain energy of $Sr_yCo_4Sb_{12}$ as a function of the filling fraction. The solid line represents a linear fit to the data.

$$\Delta E_1 = \Delta E_b + \Delta E_s, \tag{4}$$

where ΔE_b is the contribution from the extra chemical bonding between an impurity and the neighboring host atoms, and ΔE_s represents the strain energy that comes from the lattice expansion and the local strain of the host crystal environment.

The strain energy ΔE_s can be calculated in the following way. First the relaxed structure of filled skutterudite is obtained. By removing the impurity atom from the relaxed filled $CoSb_3$, an expanded and distorted $CoSb_3$ is then obtained. The total energy difference between the unstrained $CoSb_3$ and the strained $CoSb_3$ structures gives the strain energy for a particular impurity, i.e.,

$$\Delta E_s = E_{CoSb_3}(s) - E_{CoSb_3}, \tag{5}$$

where $E_{CoSb_3}(s)$ means the total energy for $CoSb_3$ with expanded and distorted structure after removing the filler atom. Figure 3 plots the strain energy as a function of the filling fraction y for $Sr_yCo_4Sb_{12}$. ΔE_s is reasonably linear in y when $y<0.5$, suggesting that the strain energy per Sr is a constant. Calculations for Ba and Yb show a similar trend in ΔE_s vs y. Therefore, the strain energy per impurity atom can be estimated from the total energy calculations for filled $CoSb_3$ at a specified y. In this paper, the filled $CoSb_3$ with filling fraction $y=0.125$ is used for the estimation of the strain energies for all impurities. The bonding contribution ΔE_b can be estimated by subtracting the strain energy ΔE_s from ΔE_1.

The lattice expansion that takes place upon an impurity atom entering the void may be regarded as an isotropic process, so that the deviation from the equilibrium position for each atom in the host structure is uniform. Assuming that the absolute deviation from the equilibrium position for each atom in the strained structure is very small, a parabolic approximation should be a good description for the strain energy,[29] i.e.,

$$\Delta E_s = \frac{1}{2} C_0 \frac{(d-d_0)^2}{d_0^2}. \tag{6}$$

The distance between the impurity I and a nearest Sb atom is used as a measure of the lattice expansion, where d_0 is the

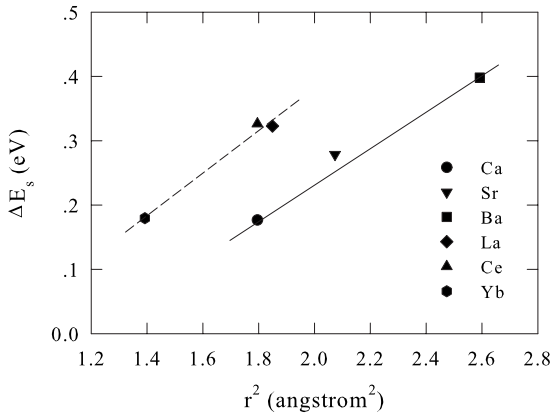

FIG. 4. Relationship between the ionic radius r of various filler impurities and the corresponding lattice strain energy ΔE_s of filled $CoSb_3$. The lines are guides for the eye.

equilibrium I-Sb distance, $d-d_0$ is the deviation from equilibrium, and C_0 is a parameter playing the role of the force constant. Because different fillers expand the lattice to different extents (depending on the ionic radius), C_0 is approximately a constant and $d-d_0$ should be proportional to the ionic radius of the impurity. Therefore, it is rational to expect that the strain energy is proportional to the square of the ionic radius for similar impurities. Figure 4 plots the relationship between ΔE_s and the square of the ionic radius (r^2) of impurities in $CoSb_3$. For alkaline-earth-metal-filled skutterudites, all impurities have almost the same valence charge (2+), and thus ΔE_s should be proportional to r^2. A linear trend (solid line) shown in Fig. 4 further corroborates the arguments.

Depending on the characteristics of chemical bonds formed between the filler impurity and the surrounding Sb atoms, the host crystal may also undergo an anisotropic structural distortion. Its contribution to the strain energy is usually complicated. It is expected that rare-earth (RE) impurities would give rise to the anisotropic strain effect because both d and f electrons have preferred bonding directions that are different from those of s electrons in alkaline earths. This may explain the relatively large strain energy of RE impurities in comparison with the alkaline-earths with comparable ionic radii. According to our calculations, there is more structural distortion of the dodecahedral Sb cages in La- and Ce-filled $CoSb_3$ than in Ca-filled $CoSb_3$, despite their nearly the same ionic radii (1.36 Å for La, 1.34 Å for Ce, and 1.34 Å for Ca).[30] Yb is a particularly interesting filler atom with a very small ionic radius (1.18 Å). Figure 4 shows that the Yb-induced strain energy is larger than that estimated from the strain energy trend of Ca-, Sr-, and Ba-filled $CoSb_3$ for a comparable ion size. Notice that the effective charges of Yb and alkaline-earths in filled $CoSb_3$ are comparable; therefore, we attribute the difference in the strain energy to the anisotropic structural distortions of REs.

Overlaps between the valence orbitals of the filler atom and those of the Sb and Co atoms at the nearest or next nearest positions are close to zero. This indicates that the chemical bonds between the filler and the host atoms are mostly ionic. Because of the charge screening effect of the irregular dodecahedral Sb cage surrounding the filler, the Coulombic interactions between the impurity and Co atoms are expected to be very weak.

The strong Coulombic interaction between the filler and Sb atoms at its nearest-neighbor positions and the weak Coulombic interaction between the filler and Co atoms at its second nearest-neighbor positions can also be revealed in the electron charge density redistribution as a consequence of the filler entering the void. The electron charge density redistribution is defined as

$$\Delta\rho = \rho_{I_yCo_4Sb_{12}} - \rho_{\square Co_4Sb_{12}} - y\rho_I, \tag{7}$$

where $\rho_{I_yCo_4Sb_{12}}$, $\rho_{\square Co_4Sb_{12}}$, and ρ_I are the electron charge density distributions of the filled skutterudite $I_yCo_4Sb_{12}$, the pure $CoSb_3$, and an isolated impurity I, respectively. Because the structure relaxes after the filler is inserted, the lattice structures for $I_yCo_4Sb_{12}$ and Co_4Sb_{12} used for the electron charge density calculations are all based on the final relaxed structure of $I_yCo_4Sb_{12}$.

Figure 5 plots $\Delta\rho$ for various filler impurities. Only results for $y=0.125$ are shown here. Calculations for higher filling fractions show the same trend. Data in Fig. 5 show that upon insertion of a filler impurity, the charge density is altered only in regions close to the boundary of the irregular dodecahedral Sb cage surrounding the filler, and around the filler impurity. Areas around the Sb atom closest to the filler show electron accumulation. Other Sb atoms that form the irregular dodecahedral cage around the filler display the same pattern of charge distribution. The accumulated electrons can only come from the filler, and thus the area around the filler is depleted of electrons. These results, along with the number of missing valence electrons obtained from the integral of the projected DOS of the impurities discussed above, clearly show that the inserted filler loses its valence electrons to the nearest-neighbor Sb atoms, leading to a strong ionic interaction.

The Co sites are not the nearest-neighbor sites to the filler and, moreover, the large carrier density in filled skutterudites results in the charge screening effect. Thus the charge distribution at the Co sites is barely affected by the presence of filler. The insertion of filler atoms does cause a small amount of electron transfer between different orbitals of the same Co atom due to the lattice strain effect upon insertion of an impurity into the lattice void and the impurity-ion-induced polarization effect. The integrated electron numbers for the s and p orbitals of the Co atom at the nearest-neighboring positions are basically unchanged upon filling, but a few electrons of Co d orbitals are lost. It is known that Co-Sb covalent bonds are determined by Co d orbitals and Sb p orbitals.[1] Because the Sb atoms are affected by a strong Coulombic interaction with the filler ion, we believe that the change of the Co electrons is also due to the electron transfer from a Co atom to an Sb atom close to the filler. The integrated electron numbers for a Co atom at the non-nearest-neighboring positions are almost equal to that of strain-free $CoSb_3$, indicating that the picture of weak long-range direct interaction between impurity and Co atoms is reasonable.

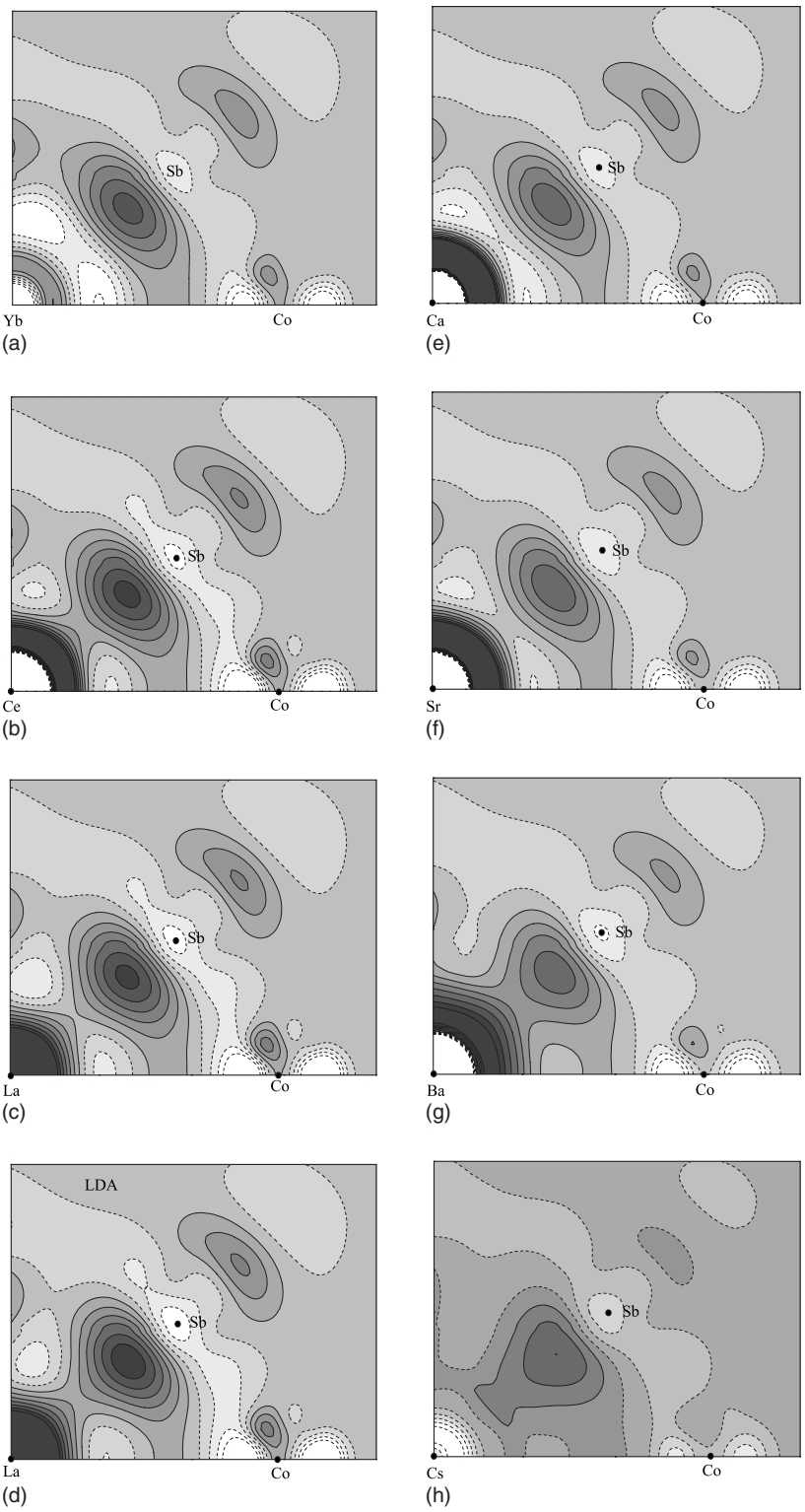

FIG. 5. Electron-density difference contour plots for the plane containing *I*, Co, and Sb atoms for (a) $Yb_{0.125}Co_4Sb_{12}$, (b) $Ce_{0.125}Co_4Sb_{12}$, (c) $La_{0.125}Co_4Sb_{12}$, (d) $La_{0.125}Co_4Sb_{12}$ using LDA, (e) $Ca_{0.125}Co_4Sb_{12}$, (f) $Sr_{0.125}Co_4Sb_{12}$, (g) $Ba_{0.125}Co_4Sb_{12}$, and (h) $Cs_{0.125}Co_4Sb_{12}$. The plot represents the space distribution of the charge density difference calculated using Eq. (7). The relatively dark area with solid lines indicates electron accumulation, and the light area with dashed lines indicates electron depletion. The black points label the positions of atoms.

The ionic radius of the filler impurity significantly affects the electron density redistribution. Figures 5(a)–5(c) and 5(e)–5(h) are arranged so that the ionic radius of the RE and alkaline-earth impurities are in ascending order, respectively. Yb has the smallest ionic radius among all RE impurities studied here. The large blank region between the Yb and Sb atoms in Fig. 5(a) suggests a rather complete electron transfer from Yb to Sb, consistent with its small lattice expansion. As the ionic radius increases from Yb to Ce, and then to La, the electron accumulation between the filled impurity and the nearest-neighboring Sb becomes more and more noticeable. This is consistent with the increased lattice expansion and increased strain energy (Fig. 4) as the ionic radius increases. A similar trend is also observed in Figs. 5(e)–5(h) for alkaline-earth-metal-filled skutterudites. It is very interesting to note that the electron density redistribution due to filling with Cs [Fig. 5(h)] is different from that for other impurities. As is well known, Cs has a very large ionic radius (1.88 Å)

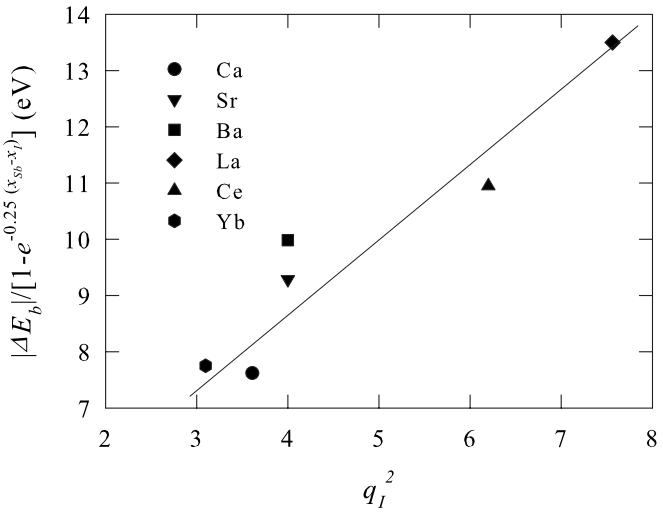

FIG. 6. Relationship among the bonding energy ΔE_b of an isolated impurity, valence charge, and electronegativity of the impurity atom in $CoSb_3$. The solid line is a guide for the eye.

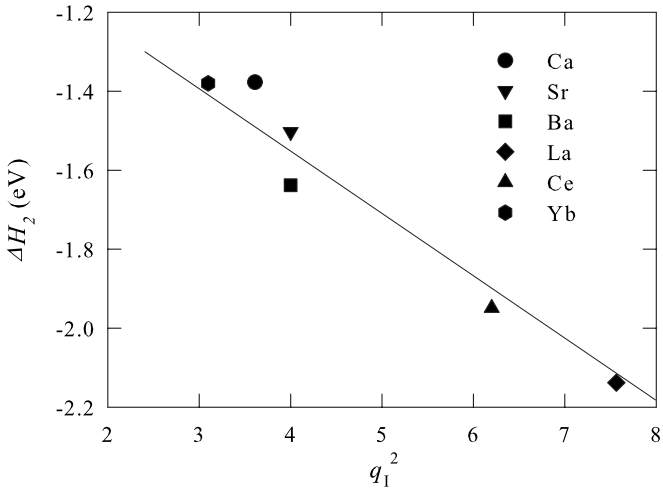

FIG. 7. Relationship between the formation energy ΔH_2 of the secondary phases and the square of filler valence. The solid line is a linear fit.

(Ref. 30) even in comparison with Ba (1.61 Å).[30] The charge redistribution pattern seems to suggest that the Cs ion is too large to fit into the void in $CoSb_3$. The Cs-filled skutterudite is unstable, and the calculated FFL for Cs in $CoSb_3$ is zero. Note that the electron density distribution for La in $CoSb_3$ calculated using LDA is also shown in Fig. 5(d) and shows the same pattern as that obtained in the GGA approach.

The overlap orbitals and electron density redistribution analysis for various impurities in $CoSb_3$ lead us to conclude that ΔE_b is mainly determined by the I-Sb interactions that are of predominantly ionic nature. Pauling proposed that the ionic character of a chemical bond is proportional to $(1-e^{-0.25(x_{Sb}-x_I)})$,[27] ΔE_b is phenomenologically approximated as

$$\Delta E_b = B_1 q_I^{\,2}(1 - e^{-0.25(x_{Sb}-x_I)}) + B_2 e^{-0.25(x_{Sb}-x_I)}. \quad (8)$$

The first and second terms represent the ionic and covalent parts of chemical bonds around an impurity I, with B_1 and B_2 being constants. The electronegativity of the filler and Sb atoms are designated as x_I and x_{Sb}, respectively. The fitted B_1 and B_2 values according to Eq. (8) are -1.80 V/e and -0.2 eV, respectively. Since B_2 is small, the second term in Eq. (8) can be neglected without altering the physical trend. This is also consistent with the picture that the I-Sb bonds are predominantly ionic in nature. Figure 6 plots $\Delta E_b/(1-e^{-0.25(x_{Sb}-x_I)})$ vs q_I^2 for all impurities. The data show a good linear relationship between the two, suggesting that Eq. (8) (without the second term) is a good approximation.

B. Factors determining ΔH_2

The crystal structures of the possible secondary phases (MSb_2) are not the same. For instance, $CaSb_2$,[31] $SrSb_2$,[32] and $BaSb_2$ (Ref. 33) crystallize in the space group $P12_1/m1$, while that for $LaSb_2$,[34] $CeSb_2$,[34] and $YbSb_2$ (Ref. 35) is $Cmcm$. There are, however, two common features amongst these secondary phases. First, the difference between the electronegativity of any one of the impurities and that of Sb atom is so large that the chemical bonds of these secondary phases are predominantly ionic. Second, they all have a similar chemical formula of ISb_2. For clarity, the formation energy of a secondary phase can be expressed as

$$\Delta H_2 = (E_{ISb_2} - 2E_{Sb} - E_I) + 2(E_{Sb} + E_{CoSb_2} - E_{CoSb_3}). \quad (9)$$

The terms in the first parentheses represent the cohesive energy of ISb_2, and the second is a constant. Due to the nearly pure ionic character of the chemical bonds in ISb_2 and in filled $CoSb_3$ between I and Sb, we assume that the charge states of the impurities in both chemical environments are approximately the same. Therefore, the term $(E_{ISb_2}-2E_{Sb}-E_I)$ should approximately be proportional to q_I^2, where q_I is the effective charge state of a filler in the void of $CoSb_3$. The formation energy for the secondary phases can be rewritten as

$$\begin{aligned}\Delta H_2 &= (E_{ISb_2} - 2E_{Sb} - E_I) + 2(E_{Sb} + E_{CoSb_2} - E_{CoSb_3}) \\ &= C_1 q^2 + C_2, \end{aligned} \quad (10)$$

where C_1 and C_2 are constants. In fact, the charge states of the impurities in ISb_2 may be slightly different from those in $CoSb_3$, and this may lead to errors in Eq. (10). Figure 7 plots the correlation between ΔH_2 and q_I^2, and it shows a reasonably good linear relationship. The fitted C_1 and C_2 values are -0.25 V/e and -0.54 eV, respectively. Equation (10) is by no means a rigorous description; we use it merely to illustrate the physical trend.

C. Filling fraction limit

1. FFL and a selection rule

Combining Eqs. (3)–(10) we have

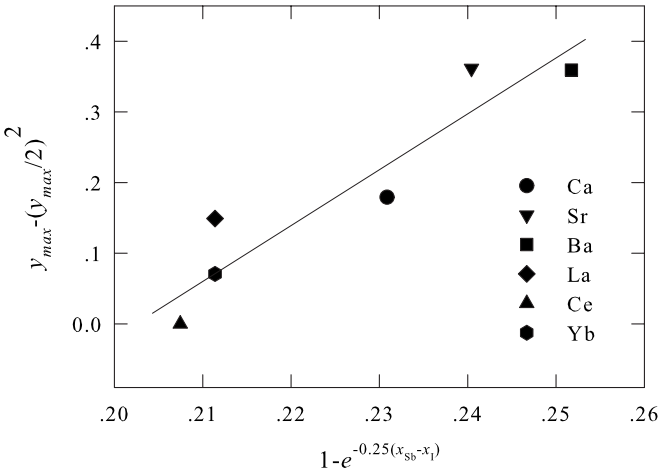

FIG. 8. Correlation between the FFLs of impurities in $CoSb_3$ and their electronegativities at absolute zero temperature.

$$y_{\max} - \left(\frac{y_{\max}}{2}\right)^2 = D_1(1 - e^{-0.25(x_{\mathrm{Sb}} - x_I)}) + D_2 + \frac{D_3 + D_4 q_I}{q_I^2}. \quad (11)$$

Quantitatively the third term on the right-hand side of Eq. (11) is much smaller than the first two terms and, therefore, can be neglected. Figure 8 shows a good linear relationship between $y_{\max} - (y_{\max}/2)^2$ and $1 - e^{-0.25(x_{\mathrm{Sb}} - x_I)}$ at 0 K. The constants D_1 and D_2 can be estimated by the linear fitting in Fig. 8. The fitted D_1 and D_2 values are 7.60 and −1.53 at absolute zero temperature, and the ratio between D_1 and D_2 is 5.7, in good agreement with the ratio between B_1 [Eq. (8)] and C_1 [Eq. (10)]. This further demonstrates that neglecting the last term on the right-hand side of Eq. (11) is reasonable.

Relationship of $y_{\max} - (y_{\max}/2)^2$ vs $1 - e^{-0.25(x_{\mathrm{Sb}} - x_I)}$ at 1000 K also shows a good linear correlation (see Fig. 4 in Ref. 19), and the fitted D_1 and D_2 values are 5.29 and −0.96, respectively. It is really surprising that FFL turns out to be sensitive to the electronegativity but not directly to the charge state of the filler ion. The experimental FFL values for Eu and Nd in $CoSb_3$ are also included in Fig. 8, and seem to be also consistent with the linear trend. By comparing the results calculated using density functional theory (Fig. 4 in Ref. 19) with the general trend shown in Fig. 8, we believe that we have unveiled an important factor determining the FFL. Because the filling fraction should be greater than zero, i.e., $y_{\max} > 0$, we may get a simple but a very useful selection rule using Eq. (11) for the formation of filled $CoSb_3$, i.e.,

$$x_{\mathrm{Sb}} - x_I > 0.80. \quad (12)$$

By inspecting the values of electronegativity of all known elements, it is found that only rare-earths, alkaline-earths, and alkaline elements can fill the voids of $CoSb_3$. Rare-earths such as La, Ce, Nd, Eu, and Yb; and alkaline-earths Ca, Sr, and Ba have been successfully inserted in the voids of $CoSb_3$. We note that the alkaline elements should also be good candidates as fillers in $CoSb_3$ because they satisfy the selection rule. We have recently demonstrated both theoretically and experimentally that *K* has very high FFL value in $CoSb_3$.[36]

2. Effect of ion radius on FFL

The extent to which the ionic radius affects the FFL in $CoSb_3$ is a complicated issue. Here we give a brief summary of how the ionic radius of the filler affects the thermodynamic stabilities of the antimonide skutterudites.

In general, ΔE_b is much larger than ΔE_s, implying that the stability of a filled skutterudite requires a strong bonding between *I* and the neighboring Sb. Crystal lattice expansion due to the insertion of the fillers into the voids of the skutterudite structure increases linearly with the ionic radius of the fillers having ionic radius between 1.34 Å and 1.61 Å.[37] Below the lower limit (1.34 Å), the size of the voids in antimonide skutterudite is too large for the fillers and the lattice expansion is governed mostly by the charge state of the filler. In contrast, fillers with ionic radii larger than the upper limit 1.61 Å (but smaller than the void radius) are too large for the voids in $CoSb_3$ and, therefore, the interaction between the filler ions and antimony atoms would lead to repulsion due to a strong overlap of the orbitals.[37] The total energy of the filled skutterudites increases sharply after the insertion of the large filler, and thus makes the system unstable. Within the range of the linear expansion, the lattice expansion and relaxation of the ionic position of the host atoms are mostly in the elastic region and do not introduce abnormally large strain energy into the system.

The increase of ionic radius of the filler impurity increases the strain energy ΔE_s and lowers the repulsive energy between the impurities ΔE_2. Therefore, the size effect of the impurity on FFL is also expected to be small, except for some special cases. Above the upper limit 1.61 Å, the electron density redistribution due to the presence of the filler in $CoSb_3$ is greatly affected by the ion radius, and a strong charge overlap occurs between the filler and antimony atoms [see Fig. 5(h)]. This makes the filled system unstable, and the strain energy becomes abnormally large while the repulsive energy between the fillers is also very high. FFL is reduced dramatically in this case. For all the filler atoms studied in this paper, Cs has the lowest electronegativity, but the largest ionic radius (1.88 Å) well above the upper limit (~1.61 Å). FFL for Cs in $CoSb_3$ is mainly determined by the size effect of the large ionic radius of Cs, and it is zero.

IV. SUMMARY AND CONCLUSIONS

We have studied the thermodynamic stability of filled skutterudites, and the filling fraction limit for Ca, Sr, Ba, La, Ce, Yb, and Cs in $CoSb_3$ using *ab initio* methods. Our theoretically predicted FFLs show excellent agreement with experimental observations. Several detailed models are proposed to explain quantitatively the bonding energy between the filler and host atoms, the lattice strain energy of the host structures, the formation energy of the secondary phases, and FFLs for various impurities in $CoSb_3$. We also systemically studied the effective charge states of the impurities in skutterudite. The calculated and experimental values agree with each other. A correlation among FFLs of the impurities in skutterudite, the effective charges, and the corresponding ionic radius is discussed. The FFL turns out to be sensitive to the filler atom's electronegativity, but not to its charge state

or the ionic radius directly. A simple selection rule for an impurity atom to be able to form a stable filled skutterudite is discovered, and it agrees quite well with the experimental observations.

ACKNOWLEDGMENTS

The authors would like to acknowledge financial support from the National Science Foundation of China and the 973 program under Grant No. 2007CB607503, and SCCAS for providing computational time on the Shenteng-6800 supercomputer. One of the authors (J.Y.) thanks Jan F. Herbst and Mark Verbrugge for continuous support and encouragement. The work is in part supported by GM and by DOE under corporate agreement Contract No. DE-FC26-04NT42278.

[1] C. Uher, in *Semiconductors and Semimetals*, edited by T. M. Tritt (Academic, San Diego, 2001), Vol. 69, p. 139, and references therein.
[2] D. T. Morelli and G. P. Meisner, J. Appl. Phys. **77**, 3777 (1995).
[3] D. T. Morelli, G. P. Meisner, B. X. Chen, S. Q. Hu, and C. Uher, Phys. Rev. B **56**, 7376 (1997).
[4] G. S. Nolas, J. L. Cohn, and G. A. Slack, Phys. Rev. B **58**, 164 (1998).
[5] V. L. Kuznetsov, L. A. Kuznetsova, and D. M. Rowe, J. Phys.: Condens. Matter **15**, 5035 (2003).
[6] G. A. Lamberton, Jr., S. Bhattacharya, R. T. Littleton IV, M. A. Kaeser, R. H. Tedstrom, T. M. Tritt, J. Yang, and G. S. Nolas, Appl. Phys. Lett. **80**, 598 (2002).
[7] G. S. Nolas, M. Kaeser, R. T. Littleton IV, and T. M. Tritt, Appl. Phys. Lett. **77**, 1855 (2000).
[8] B. C. Sales, B. C. Chakoumakos, and D. Mandrus, Phys. Rev. B **61**, 2475 (2000).
[9] M. Puyet, B. Lenoir, A. Dauscher, M. Dehmas, C. Stiewe, and E. Müller, J. Appl. Phys. **95**, 4852 (2004); M. Puyet, A. Dauscher, B. Lenoir, M. Dehmas, C. Stiewe, E. Müller, and J. Hejtmanek, *ibid.* **97**, 083712 (2005).
[10] L. D. Chen, T. Kawahara, X. F. Tang, T. Goto, T. Hirai, J. S. Dyck, W. Chen, and C. Uher, J. Appl. Phys. **90**, 1864 (2001); J. S. Dyck, W. Chen, C. Uher, L. Chen, X. F. Tang, and T. Hirai, *ibid.* **91**, 3698 (2002).
[11] G. S. Nolas, H. Takizawa, T. Endo, H. Sellinschegg, and D. C. Johnson, Appl. Phys. Lett. **77**, 52 (2000).
[12] G. S. Nolas, J. Yang, and Hirotsugu Takizawa, Appl. Phys. Lett. **84**, 5210 (2004).
[13] M. Llunell, P. Alemany, S. Alvarez, V. P. Zhukov, and A. Vernes, Phys. Rev. B **53**, 10605 (1996).
[14] J. L. Feldman and D. J. Singh, Phys. Rev. B **53**, 6273 (1995).
[15] D. J. Singh and W. E. Pickett, Phys. Rev. B **50**, 11235 (1994).
[16] D. J. Singh and I. I. Mazin, Phys. Rev. B **56**, R1650 (1997).
[17] O. M. Løvvik and Ø. Prytz, Phys. Rev. B **70**, 195119 (2004).
[18] L. Bertin and C. Gatti, J. Chem. Phys. **121**, 8983 (2004).
[19] X. Shi, W. Zhang, L. D. Chen, and J. Yang, Phys. Rev. Lett. **95**, 185503 (2005).
[20] G. Kresse and D. Joubert, Phys. Rev. B **59**, 1758 (1999); P. E. Blöchl, *ibid.* **50**, 17953 (1994).
[21] G. Kresse and J. Furthmüller, Phys. Rev. B **54**, 11169 (1996); G. Kresse and J. Hafner, *ibid.* **47**, 558 (1993).
[22] J. P. Perdew, K. Burke, and M. Ernzerhof, Phys. Rev. Lett. **77**, 3865 (1996).
[23] D. Spišák and J. Hafner, Phys. Rev. B **67**, 235403 (2003); O. Dulub, U. Diebold, and G. Kresse, Phys. Rev. Lett. **90**, 016102 (2003).
[24] W. Zhang, J. R. Smith, and A. G. Evans, Acta Mater. **50**, 3803 (2002).
[25] X. Y. Zhao, X. Shi, L. D. Chen, W. Q. Zhang, W. B. Zhang, and Y. Z. Pei, J. Appl. Phys. **99**, 053711 (2006).
[26] F. Grandjean, G. J. Long, B. Mahieu, J. Yang, G. P. Meisner, and D. T. Morelli, J. Appl. Phys. **94**, 6683 (2003).
[27] L. Pauling, *The Nature of the Chemical Bond*, 3rd ed. (Cornell University Press, Ithaca, 1960).
[28] L. D. Chen (unpublished).
[29] W. A. Harrison, *Electronic Structure and the Properties of Solids* (W. H. Freeman, New York, 1980).
[30] R. D. Shannon, Acta Crystallogr., Sect. A: Cryst. Phys., Diffr., Theor. Gen. Crystallogr. **A32**, 751 (1976).
[31] K. Deller and B. Eisenmann, Z. Anorg. Allg. Chem. **425**, 104 (1976).
[32] K. Deller and B. Eisenmann, Z. Naturforsch. B **31**, 1146 (1976).
[33] B. Eisenmann, C. Gieck, and U. Roessler, Z. Kristallogr. - New Cryst. Struct. **216**, 36 (2001).
[34] R. Wang and H. Steinfink, Inorg. Chem. **6**, 1685 (1967).
[35] R. Wang, R. Bodnar, and H. Steinfink, Inorg. Chem. **5**, 1468 (1966).
[36] W. Zhang, X. Shi, Z. G. Mei, Y. Xu, L. D. Chen, J. Yang, and G. P. Meisner, Appl. Phys. Lett. **89**, 112105 (2006).
[37] X. Shi, Ph.D. thesis, Shanghai Institute of Ceramics, Chinese Academy of Sciences, Shanghai, China, 2005.